AFRL-RW-EG-TP-2011-015

Observation of a Minimum Reaction Initiation Threshold in Ball-Milled Ni + Al Under High-Rate Mechanical Loading

STINFO COPY

Eric B. Herbold
Naresh N. Thadhani

School of Materials Science and Engineering
Georgia Institute of Engineering
Atlanta, GA 30332

Jennifer L. Jordan

Air Force Research Laboratory
Munitions Directorate/Ordnance Division
Energetic Materials Branch (AFRL/RWME)
Eglin AFB, FL 32542-5910

February 2011

Interim Report

This paper was published in the Journal of Applied Physics, March 2011.

AIR FORCE RESEARCH LABORATORY, MUNITIONS DIRECTORATE

Air Force Materiel Command ■ United States Air Force ■ Eglin Air Force Base

This page intentionally left blank

NOTICE AND SIGNATURE PAGE

Using Government drawings, specifications, or other data included in this document for any purpose other than Government procurement does not in any way obligate the U.S. Government. The fact that the Government formulated or supplied the drawings, specifications, or other data does not license the holder or any other person or corporation; or convey any rights or permission to manufacture, use, or sell any patented invention that may relate to them.

Qualified requestors may obtain copies of this report from the Defense Technical Information Center (DTIC) <http://www.dtic.mil/dtic/index.html>.
.

AFRL-RW-EG-TP-2011-015 HAS BEEN REVIEWED AND IS APPROVED FOR PUBLICATION IN ACCORDANCE WITH ASSIGNED DISTRIBUTION STATEMENT.

FOR THE DIRECTOR:

//Original Signed//	//Original Signed//	//Original Signed//
HOWARD G. WHITE, PhD	JEFFREY D. KUHN, MAJ, PhD	JENNIFERL. JORDAN, PhD
Technical Advisor	Branch Chief	Project Manager
Ordnance Division	Energetic Materials Branch	Energetic Materials Branch

This report is published in the interest of scientific and technical information exchange, and its publication does not constitute the Government’s approval or disapproval of its ideas or findings.

This page intentionally left blank

REPORT DOCUMENTATION PAGE

Form Approved
OMB No. 0704-0188

1. REPORT DATE *(DD-MM-YYYY)*	**2. REPORT TYPE**	**3. DATES COVERED** *(From - To)*
04-2011	Interim	October 2009 – March 2011

4. TITLE AND SUBTITLE

Observation of a Minimum Reaction Initiation Threshold in Ball-Milled Ni + Al Under High-Rate Mechanical Loading

5a. CONTRACT NUMBER

5b. GRANT NUMBER

5c. PROGRAM ELEMENT NUMBER
62102F

6. AUTHOR(S)

Eric B. Herbold, Naresh N. Thadhani, Jennifer L. Jordan

5d. PROJECT NUMBER
4347

5e. TASK NUMBER
95

5f. WORK UNIT NUMBER
05

7. PERFORMING ORGANIZATION NAME(S) AND ADDRESS(ES)

School of Materials Science and Engineering
Georgia Institute of Technology
Atlanta, GA 30332

Air Force Research Laboratory
Munitions Directorate
Ordnance Division
Energetic Materials Branch
Eglin AFB, FL 32542-5910

8. PERFORMING ORGANIZATION REPORT NUMBER

AFRL-RW-EG-TP-2011-015

9. SPONSORING / MONITORING AGENCY NAME(S) AND ADDRESS(ES)

Air Force Research Laboratory, Munitions Directorate
Ordnance Division
Energetic Materials Branch (AFRL/RWME)
Eglin AFB FL 32542-5910
Technical Advisor: Dr. Jennifer L. Jordan

10. SPONSOR/MONITOR'S ACRONYM(S)
AFRL-RW-EG

11. SPONSOR/MONITOR'S REPORT NUMBER(S)
Same as Block 8

12. DISTRIBUTION / AVAILABILITY STATEMENT

Distribution A: Approved for public release; distribution unlimited. Approval Confirmation 96 ABW/PA # 96ABW-2010-0451, Dated August 12, 2010

13. SUPPLEMENTARY NOTES

DISTRIBUTION STATEMENT INDICATING AUTHORIZED ACCESS IS ON THE COVER PAGE AND BLOCK 12 OF THIS FORM.

14. ABSTRACT

Two types of microstructurally distinct ball-milled Ni+Al powder compacts are characterized for the investigation of reaction initiation threshold under high-rate mechanical loading using a modified rod-on-anvil Taylor impact-test setup. It is observed that the kinetic energy threshold for reaction decreases to a minimum then increases with milling time. It is also observed that the kinetic energy required for reaction initiation is lower for the 95% theoretical maximum density (TMD) ball-milled powder compacts than for the 65% theoretical maximum density (TMD) compacts. The results are discussed on the basis of competing effects of reactivity enhancement and deformability reduction caused by prior ball-milling of the powder mixtures. © 2011 American Institute of Physics.

15. SUBJECT TERMS
Nickel powder, aluminum powder, ball mill, reaction

16. SECURITY CLASSIFICATION OF:			**17. LIMITATION OF ABSTRACT**	**18. NUMBER OF PAGES**	**19a. NAME OF RESPONSIBLE PERSON**
a. REPORT	**b. ABSTRACT**	**c. THIS PAGE**			Jennifer L. Jordan
UNCLASSIFIED	UNCLASSIFIED	UNCLASSIFIED	UL	8	**19b. TELEPHONE NUMBER** *(include area code)* 850-882-8992

Standard Form 298 (Rev. 8-98)
Prescribed by ANSI Std. Z39.18

This page intentionally left blank

Observation of a minimum reaction initiation threshold in ball-milled Ni+Al under high-rate mechanical loading

Eric B. Herbold,[1,a)] Naresh N. Thadhani,[1] and Jennifer L. Jordan[2]
[1]*School of Materials Science and Engineering, Georgia Institute of Technology, Love Manufacturing Building, 771 Ferst Drive, Atlanta, Georgia 30332, USA*
[2]*High Explosives Research and Development Branch, Munitions Directorate, Air Force Research Laboratory, Eglin AFB, Florida 32542, USA*

(Received 1 November 2010; accepted 21 December 2010; published online 29 March 2011)

Two types of microstructurally distinct ball-milled Ni+Al powder compacts are characterized for the investigation of reaction initiation threshold under high-rate mechanical loading using a modified rod-on-anvil Taylor impact-test setup. It is observed that the kinetic energy threshold for reaction decreases to a minimum then increases with milling time. It is also observed that the kinetic energy required for reaction initiation is lower for the 95% theoretical maximum density (TMD) ball-milled powder compacts than for the 65% theoretical maximum density (TMD) compacts. The results are discussed on the basis of competing effects of reactivity enhancement and deformability reduction caused by prior ball-milling of the powder mixtures. © *2011 American Institute of Physics*. [doi:10.1063/1.3549822]

Chemical reactions in powder materials have been an active area of investigation in recent years for synthesis of novel compounds by various methods of dynamic loading or processing techniques involving relatively "fast"[1–12] or "moderate"[13–16] reaction rates. Investigations of "fast" reactions include laser-induced desorption ionization in metal-metal-oxides[12] and those resulting from shock-compression of powder mixtures.[1–11] The latter are characterized by "shock-induced" chemical reactions occurring within the time-scale of the shock duration: typically on the order of several microseconds. In contrast, "shock-assisted" chemical reactions initiate following the peak pressure state during the thermal equilibration time scale[2,3,7,9] and are being investigated for applications relevant to energetic materials.[17] Mechanisms leading to shock-induced chemical reactions in powders, whether mechanochemical or thermomechanical in nature, vary as a function of the intrinsic and extrinsic properties of materials and their loading conditions.[18] For example, pore collapse,[19] localized melting,[10,11] and disparate material properties may affect the occurrence of reaction. In contrast, the synthesis of intermetallic compounds at longer time-scales resulting from gradual and explosive reactions at the grain level has been observed in powders processed using high-energy ball-milling.[13–16]

Self-sustaining high-temperature synthesis (SHS) reactions in intermetallic-forming systems result in the release of large amounts of heat and occur during ball-milling of Ni and Al powders mixed in an equiatomic ratio.[13,14] Arrested reactive milling (ARM) techniques halt the milling process prior to SHS reaction resulting in a fine blend of constituent powders.[16] Typical ARM materials have a layered microstructure at length-scales on the order of tens to a few hundred nm. During thermal analysis the apparent temperature threshold for reaction of these powders have been shown to decrease with increased milling time at the expense of total energy output.[9]

A recent investigation of shock induced chemical reactions in ball-milled Ni+Ti powder shows that increased milling times raises its crush-strength due to strain hardening.[9] Correspondingly, the extent of reaction observed during shock-compression decreased with increasing ball-milling time. These results illustrate reduced reactivity of ball-milled powder mixtures during shock-compression (uniaxial-strain loading) despite a more intimately mixed powder.[6]

Here, the reaction/combustion characteristics of ball-milled Ni+Al (each at 50 at.%) powders are investigated using modified rod-on-anvil Taylor impact experiments with pressed pellets that vary in microstructure and density, mounted onto Cu rods, and impacted against a high-strength anvil. Mechanisms related to impact induced initiation of gasless chemical reactions are important for applications involving novel energetic materials. The high strain-rates (10^4–10^5 s^{-1}) and combined loading conditions indicate whether the reaction occurs during compaction, shear or severe plastic straining in the axial and lateral directions.

The energy level required for initiation and the amount released during reaction vary as a function of milling time. Here, ball-milled Ni+Al powder compacts are formed from powders milled in a hardened steel vial with Ar in a SPEX-8000 ball-mill with temperature control. Two different material types, distinguished by the initial size of the powder (designated SARM1 and SARM2), are employed to investigate the role of ball-milling time, powder grain microstructure, and the density of the compacts. Differences in the single-grain microstructure are produced by milling 50 μm Al (H50, Valimet, Inc.) and 5–15 μm Ni (Alfa-Aesar) for SARM1 compared to 2 μm Al (H2, Valimet, Inc.) and 100 μm Ni ($-150+200$ mesh, Alfa-Aesar) for SARM2. Both powder types are milled with 7.94 mm stainless steel balls. The averaged time to reaction (t_R) for each powder is 9959 ± 862 s for SARM1 and 12632 ± 988 s for SARM2

a)Author to whom correspondence should be addressed. Electronic mail: herbold1@llnl.gov.

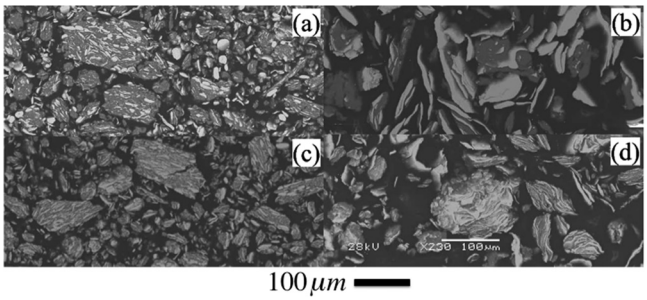

FIG. 1. Micrographs of the ball-milled powder particles (Ni is light gray and Al is dark gray). (a) The Ni+Al powder (type SARM1) milled to $0.35t_R$. (b) SARM2 powder milled to $0.35t_R$. (c) SARM1 powder milled to $0.65t_R$. (d) SARM2 powder milled to $0.65t_R$.

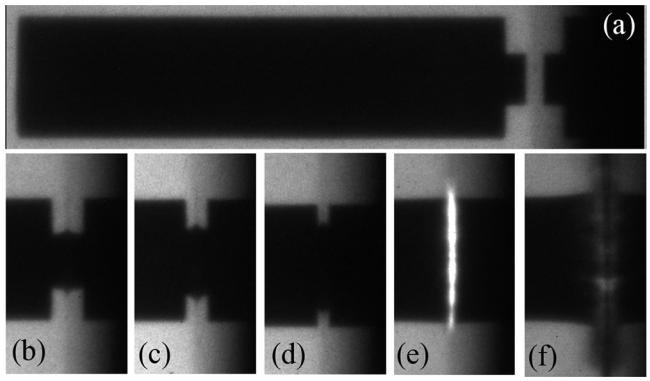

FIG. 2. Impact of a SARM1 pellet milled for $0.35t_R$ (#1–12, 81% dense) at 342 m/s. (a) $t=0$ μs: The reflection of the rod and pellet are shown on the steel impact plate. (b)–(d) $t=3$–5 μs: the ball-milled pellet has impacted the steel plate and continues to deform. (e) $t=5.5$ μs: A bright "flash" is observed indicating reaction. (f) $t=7$ μs: The Cu sabot has contacted the steel anvil and powder has escaped from the sides of the projectile.

and was determined by repeating the ball milling procedure three times with 10 g of powder until reaction was detected by thermocouples attached to the outside of the vial. Subsequent batches of each mixture were produced under identical milling conditions for times corresponding to 35% and 65% of the averaged t_R for the impact tests.

The differences in microstructure between the two unsieved powders are compared in Fig. 1. Figure 1(a) shows SARM1 powder milled to $0.35t_R$. There are moderately deformed Ni particles within the Al matrix, as well as small amounts of Ni particles dispersed between sub-micron layers of Al. Figure 1(b) shows SARM2 powder milled to $0.35t_R$. Here the Ni particles are initially much larger than in (a) and are flattened with the soft Al particles resulting in a relatively coarse laminate particle. Figure 1(c) shows that the microstructure shown in Fig. 1(a) becomes a highly refined laminate structure when milled for $0.65t_R$. This is also apparent in Fig. 1(d) where the flakelike microstructure is refined when milled for $0.65t_R$ compared with Fig. 1(b). The microstructures of the individual grains in Fig. 1(c) and 1(d) look very similar in laminate thickness. However, comparing Fig. 1(a) and 1(b) the microstructural difference between individual grains suggests that a finer laminate structure (and higher contact surface area) is achieved with SARM2 powder as shown in (b) as opposed to that with small, hard Ni particles in SARM 1 as is apparent in (a).

The impact experiments are performed in air using a modified rod-on-anvil Taylor test setup.[20] The 3.17 mm diameter pellets are mounted to a 7.62 mm diameter, 38.1 mm long Cu rod (glued with cyanoacrylate glue forming ~10–20 μm thick layer) that comprised the projectile for impact against a high-strength steel anvil with hardness Rc 46 ground to 16G. The length of the pellets range from 1.09–1.75 mm depending on the initial amount of powder and final density. SARM1 and SARM2 powders were sieved to $-140+230$ mesh (63–106 μm) and pressed to 65–95% of the theoretical maximum density (TMD), which is 5.167 g/cm^3 for Ni+Al.

An experiment using a SARM1 pellet at 73% dense is shown in Fig. 2 where the projectile is fired at a measured speed of 342 m/s. The projectile is shown prior to impact in Fig. 2(a) at $t=0$ μs and (b)–(f) show various stages of deformation and reaction. In Fig. 2(b) ($t=3$ μs) the sides of the cylindrical pellet, on average, form an angle with the steel plate that remains relatively constant in Figs. 2(c) and 2(d) (see the last two columns for $\dot{\alpha}$ in Table I). Pellet measurements from Fig. 2 are listed in Table I where the parameter h is the pellet height, d_1 is the diameter at the Cu sabot, d_2 is the diameter at the anvil, $D=(d_2-d_1)/2$, and α is the averaged angle of the side of the cylinder. There are two distinct high-rate loading conditions following impact. Considering the measured shear ($\dot{\alpha}$) and axial ($\dot{\varepsilon}_z$) strain rates, the first stage of pellet deformation is dominated by compaction and a relatively high shear strain rate followed by the second stage involving mainly high axial and radial ($\dot{\varepsilon}_{r1}$ and $\dot{\varepsilon}_{r2}$) strain rates. Figure 2(e) shows a bright "flash" of light as the Cu sabot contacts the anvil, which is an indication of the fast reaction in the ball-milled Ni+Al powder pellet. The reaction propagates into a powder dust cloud shown in Fig. 2(f). Each experimental image indicating reaction occurred at the latter stage where the particles have dynamically deformed by an averaged axial and lateral strain of approximately 0.8 (see the last column for ε_z, ε_{r1}, and ε_{r2} in Table I), though values of local strain at the scale of the particle are likely higher.

In Fig. 3 the kinetic energy of the Cu sabot and pellet is plotted as a function of (a) time of ball-milling and (b) the pressed density of the two types of sieved powders. In both (a) and (b) the open and closed markers (i and l for SARM1 and ▽ and ▼ for SARM2) indicate no reaction or a distinct 'flash' of light across the width of the pellet as seen in Fig. 2(e), indicating reaction before the sabot hit the anvil, respectively. The markers at $t=0$ s correspond to as-blended (non-milled) 92% dense Ni+Al powder pellet based on the results of our prior work.[20]

In Fig. 3, curves (1)–(2) are trendlines indicating the dependence of impact-initiated reaction energy on prior ball-milling time decreases to a minimum around $t_{\min}=0.35t_R$ and then increases with milling time for both powders. Such a trend is due to the competition of two effects. First, ball-milling creates fresh reactant surfaces to be brought into contact, thereby enhancing the reactivity of the powders. Further milling work-hardens the reactants and creates localized interfacial reactions making it more difficult for subsequent impact-initiated reactions. This indicates an optimum time exists for arrested reactive milled powders that can provide the highest sensitivity of impact-initiated reactions.

TABLE I. Pellet measurements from Fig. 2. The parameter h is the pellet length (ε_z is the engineering strain), d_1 (ε_{r1}) is the diameter (eng. strain) at the Cu sabot, d_2 (ε_{r2}) is the diameter (eng. strain) at the anvil, $D=(d_2-d_1)/2$, and α is the angle of the side of the cylinder [$\alpha=\text{atan}(D/h)$].

Figure 2 part	(a)	(b)	(c)	(d)
t (μs)	0 - 1.41[a]	3	4	5
h (mm)	1.27	0.964	0.590	0.250
d_1 (mm)	3.17	3.26	4.23	5.29
d_2 (mm)	3.17	4.11	4.82	5.60
D (mm)	0	0.425	0.295	0.155
α (rad.)	0	0.415	0.464	0.555
ε_z	0	0.241	0.535	0.803
ε_{r1}	0	0.028	0.334	0.669
ε_{r2}	0	0.297	0.521	0.767
$\dot{\alpha}(10^6\ \text{s}^{-1})$	0	0.26	0.05	0.09
$\dot{\varepsilon}_z(10^6\ \text{s}^{-1})$	0	0.19	0.29	0.27
$\dot{\varepsilon}_{r1}(10^6\ \text{s}^{-1})$	0	0.018	0.306	0.334
$\dot{\varepsilon}_{r2}(10^6\ \text{s}^{-1})$	0	0.186	0.224	0.246

[a]This estimate is based on the velocity of 342 m/s of the projectile and a gap of 0.482 mm shown in Fig. 2(a). Spatial measurements are within 4 pixels or ±0.12 mm.

However, for increased milling times shown in Fig. 3(a), the apparent reaction threshold appears at the same level of energy at $0.65t_R$ though the powders were milled for different amounts of time, respectively, and may have different levels of strain-hardening given their initial sizes. With the same milling conditions (stoichiometric and charge ratio, milling media, temperature) the energy required for initiation of reaction of the SARM1 and SARM2 may tend to a constant value independent of milling time.

In Fig. 3(b) the kinetic energy is plotted against the pressed density of the pellet for SARM1 and SARM2 milled to $0.35t_R$. The reaction is initiated at lower impact energies as the density of the pellet increases, which may be linked to the amount of load carried by the pellet. The low-density sample may dissipate energy during the compaction process, reducing bulk distributed deformation, which requires higher threshold energy (see Table I at later times). The difference in threshold values between the two materials when comparing Figs. 3(a) and 3(b) suggests that the reaction threshold depends on the density and powder microstructure in these dynamic tests for similar milling conditions.

The dependence of air or vacuum environments on the impact initiation thresholds of long PTFE/Al composite rods show that first light occurs almost twice as fast in air as in vacuum at the same impact stress, suggesting that particle size effects are less important in experiments surrounded by air.[21] Here, however, the dependence of the threshold energy on the milling time is strongly linked to microstructural differences and the results shown in Fig. 3 indicate that these differences are prevalent even in the presence of air.

Ball-milled Ni+Al powder compacts were characterized for the investigation of reaction threshold in modified Taylor impact tests. The kinetic energy (impact velocity) required for the observation of fast reaction decreases as fresh surfaces of the constituents are in close contact with minimal strain hardening and then increase due to the strain-hardening of the powder grains. There is an optimal milling time

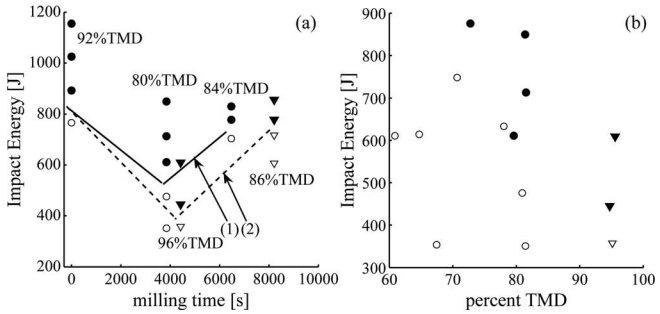

FIG. 3. The kinetic energy of the Cu sabot and pellet is plotted as a function of (a) milling time and (b) percent TMD of the Ni+Al pellet. The open markers (○ for SARM1 and ▽ for SARM2) indicate no reaction. The closed markers indicate a distinct reaction before the sabot hits the anvil. Curves (1) and (2) correspond to SARM1 and SARM2 respectively. The average density (with the first standard deviation less than 2%) is shown above or below each column of data. (b) The impact energy threshold for SARM1 and SARM2 milled to $0.35t_R$, decreases for increasing pellet density.

related to a minimum energy located around $0.35t_R$ for these materials, which is related to grain microstructure as indicated by its appearance. The energy required for reaction decreases with increasing pellet density, which is attributed to the balance of energy between the compaction process and bulk distributed deformation of the powder particles.

E.B.H. thanks the Florida Institute for Research in Energetics (FIRE) for support, J.M. Scott for ball-mill modifications and Spencer Vore for validating threshold conditions for as-blended powders. This work was supported by Eglin AFB (task-order FA-8651-08-D-0108) contracted to the University of Florida and sub-contracted to the Georgia Tech Research Institute. Partial support provided by ONR/MURI Grant No. N000147-07-1-0740.

[1]A. N. Dremin and O. N. Bruesov, Russ. Chem. Rev., **37**, 392 (1968).
[2]Y. Horie, "Shock-induced chemical reactions in inorganic powder mixtures," in *Shock Waves in Materials Science*, edited by A.B. Sawaoka (Springer-Verlag, Tokyo, 1993).
[3]N. N. Thadhani, J. Appl. Phys. **76**, 2129 (1994).
[4]Y. Yang, R. D. Gould, Y. Horie, and K. R. Iyer, Appl. Phys. Lett. **70**, 3365 (1997).
[5]V. F. Nesterenko, *Dynamics of Heterogeneous Materials* (Springer-Verlag, New York, 2001).
[6]N. N. Thadhani, T. Aizawa, "Materials issues in shock compression-induced chemical reactions in porous solids," in *High-Pressure Shock Compression of Solids IV*, edited by L. Davison, Y. Horie, M. Shahinpoor (Springer-Verlag, New York, 1997).
[7]K. S. Vandersall and N. N. Thadhani, J. Appl. Phys. **94**, 1575 (2003).
[8]V. I. Levitas, Phys. Rev. B **70**, 184118 (2004).
[9]X. Xu and N. N. Thadhani, J. Appl. Phys. **96**, 2000 (2004).
[10]M. A. Meyers, L.-H. Yu, and K. S. Vecchio, Acta Metall. Mater. **42**, 715 (1994).
[11]T. Vreeland, Jr., K. Montilla, and A. H. Mutz, J. Appl. Phys. **82**, 2840 (1997).
[12]M. L. Mileham, M. P. Kramer, and A. E. Stiegman, J. Phys. Chem. C, **111**, 16883 (2007).
[13]M. Atzmon, Phys. Rev. Lett. **64**, 487 (1990).
[14]F. Cardellini, G. Mazzone, and M. Vittori Antisari, Acta Mater. **4**, 1511 (1996).
[15]C. C. Koch, NanoStruct. Mater. **9**, 13 (1997).
[16]M. Schoenitz, T. Ward, and E. L. Dreizin, *Proceedings of the Materials Research Society* (Mater. Res. Soc., Warrendale, PA., 2004), Vol. 800, pp. 85–90, AA2.6.
[17]R. G. Ames, *Proceedings of the Materials Research Society* (Mater. Res. Soc., Warrendale, PA., 2006), Vol. 896, pp. 123–132.
[18]D. E. Eakins and N. N. Thadhani, Int. Mater. Rev. **54**, 181 (2009).
[19]M. M. Carroll and A. C. Holt, J. Appl. Phys. **43**, 1626 (1972).
[20]S. W. Du and N. N. Thadhani, AIP Conf. Proc. **1195**, 474 (2009).
[21]W. Mock, Jr. and J.T. Drotar, AIP Conf. Proc. **955**, 971 (2007).

DISTRIBUTION LIST
AFRL-RW-EG-TP-2011-015

*Defense Technical Info Center
8725 John J. Kingman Rd Ste 0944
Fort Belvoir VA 22060-6218

AFRL/RWME (6)
AFRL/RWOC-1 (STINFO Office)